Classical and semiclassical treatments of highly charged ions + H(1s) collisions

L. F. Errea, Clara Illescas, L. Méndez, B. Pons*, A. Riera, J. Suárez

Laboratorio Asociado al CIEMAT de Física Atómica y Molecular en Plasmas de Fusión.
Departamento de Química, Universidad Autónoma de Madrid, Madrid-28049, Spain
* *CELIA (UMR CNRS), Université de Bordeaux I, 351 Cours de Libération, 33405 Talence Cedex, France*

Abstract

We present impact-parameter classical trajectory Monte-Carlo and molecular close-coupling calculations for total and partial cross sections for Ne^{10+}, Ar^{+18} + H(1s) collisions, which have recently become of interest in fusion plasma research.

1 Introduction

Density diagnostics of core plasmas in tokamak reactors is currently carried out by applying charge exchange spectroscopy techniques; in these experiments one measures the intensity of emission lines of the ions formed after charge exchange between highly charged ions and neutral beams. In particular, NeX lines in the visible region (n=10-9, 11-10, 12-11, 13-12, 14-12, 15-13 and 16-14) are considered in new experiments on ASDEX-U during the present campaign. Ar is also proposed as a diagnostics species for the 2005 campaign. In this case, the n-shells giving $\Delta n = 1$ transitions in the visible are n=15, 16, 17. These diagnostics require the knowledge of accurate state-selective cross sections for electron capture reactions between highly charged ions and H at impact energies about 40 keV/amu, and the aim of the present work is to calculate electron capture cross sections for Ne^{10+} and Ar^{18+} collisions with H.

In previous works [6,7] we have analyzed the application of semiclassical close-coupling and classical CTMC to evaluate electron capture (EC) and ionization cross sections for Li^{3+} and Ne^{10+} collisions with H(1s). This study shows that

the use of an extended molecular basis (including pseudostates) and an improved initial distribution in the CTMC method allows to smoothly join the total cross sections from both calculations, which allows us to cover a large range of impact energies, although the agreement between both methods is less satisfactory for partial cross section at low values of n. In the present work, we extend the application of these methods to Ne^{10+} and Ar^{18+}, including the excited n levels required in fusion applications. Atomic units are employed unless otherwise stated.

2 Close-Coupling and CTMC methods

The two methods employed in this work are based on the impact parameter approximation [3], in which the internuclear vector $\mathbf{R}$ follows rectilinear trajectories, $\mathbf{R}(t) = \mathbf{b} + \mathbf{v}t$, with constant values of the velocity $\boldsymbol{v}$ and impact parameter $\boldsymbol{b}$. In the semiclassical treatment, the electronic motion is described by the time-dependent Schrödinger equation:

$$(H - i\frac{\partial}{\partial t})\Psi(\mathbf{r}, v, b, t) = 0 \tag{1}$$

where H is the fixed-nuclei Born-Oppenhemier Hamiltonian:

$$H = -\frac{1}{2}\nabla^2 - \frac{Z}{r_A} - \frac{1}{r_H} \tag{2}$$

and $\mathbf{r}_{A,H}$ are the electron position vectors relative to nuclei A^{Z+} and H^+, respectively. The time derivative is taken by keeping fixed the electron position vector $\mathbf{r}$ with respect to an origin of coordinates that is situated on an intermediate point of the internuclear axis.

In the close-coupling formalism, we solve eq. (1) by expanding Ψ in terms of bound eigenfunctions χ_k of the electronic Hamiltonian H, called one-electron diatomic molecule (OEDM) orbitals [19]:

$$\Psi(\mathbf{r}, v, b, t) = e^{iU(\mathbf{r},t)} \sum_k a_k(v, b, t)\chi_k(\mathbf{r}, R)e^{-i\int_0^t E_k(t')dt'} \tag{3}$$

where $U(\mathbf{r}, t)$ is the common translation factor (CTF) (see [5]), whose explicit form can be found in ref. [4].

Substitution of the ansatz (3) in Eq. (1) leads to a set of differential equations for the expansion coefficients $a_k(v, b, t)$, which are integrated up to time t_{max},

obtaining the capture and excitation transition amplitudes $a_{nlm}^{A,H}(v,b,t\to\infty)$ (see [6] and references therein). Finally, the cross section to a specific final (n,l,m) state is given by:

$$\sigma_{nlm}^{A,H}(v) = 2\pi \int |a_{nlm}^{A,H}(v,b,t\to\infty)|^2 b db. \tag{4}$$

In the impact parameter CTMC formalism, the electron dynamics is described, for each nuclear trajectory (v,b), through a set of N independent trajectories $\{\mathbf{r}_j(t)\}$ whose statistical phase-space distribution

$$\rho(\mathbf{r},\mathbf{p},v,b,t) = \frac{1}{N}\sum_{j=1}^{N}\delta(\mathbf{r}-\mathbf{r}_j(t))\delta(\mathbf{p}-\mathbf{p}_j(t)) \tag{5}$$

satisfies the Liouville equation

$$\frac{\partial\rho(\mathbf{r},\mathbf{p},v,b,t)}{\partial t} = -[\rho(\mathbf{r},\mathbf{p},v,b,t),H]. \tag{6}$$

To describe the initial H(1s) state, we have employed both, a microcanonical distribution [1]

$$\rho(\mathbf{r},\mathbf{p},v,b,t\to-\infty) = \frac{1}{8\pi^3}\delta\left(\frac{p^2}{2}-\frac{1}{r}+\frac{1}{2}\right) \tag{7}$$

and a hydrogenic distribution [9], which improves the description of the spatial density with regard to eq. (7) (without damaging seriously the momentum one), defined as superposition of M microcanonical functions:

$$\rho(\mathbf{r},\mathbf{p},v,b,t\to-\infty) = \sum_{k=1}^{M}\frac{(-2\varepsilon_k)^{5/2}}{8\pi^3}\,a_k\,\delta\left(\frac{p^2}{2}-\frac{1}{r}-\varepsilon_k\right) \tag{8}$$

where the energies ε_k and weights a_k are chosen so as to achieve good approximations to the quantum densities.

The substitution of eq. (5) in (6) yields the Hamilton equations for the evolution of the N independent trajectories, that are integrated up to time t_{max}. The ionizing part ρ_i of the classical distribution is obtained at the end of the collision under the atomic energy conditions $\{E_T=\mathbf{p}^2/2-1/r>0, E_P=1/2(\mathbf{p}-\mathbf{v})^2-Z/|\mathbf{r}-\mathbf{b}-\mathbf{v}t_{max}|>0\}$ while for the capture part ρ_c, $\{E_T>0, E_P<0\}$. Moreover, the classical phase space of the capture electrons is partitioned into exclusive subspaces, each of them being associated with a quantum state with definite n and l. The partition is made so that the relative volume of a given

subspace matches the multiplicity of the corresponding quantum shell [2]; all the electronic trajectories which end up with an energy $E_P = -Z^2/2n_c^2$ and an angular momentum $l_c = |(\mathbf{r}-\mathbf{b}-\mathbf{v}t_{max})\wedge(\mathbf{p}-\mathbf{v})|$ relative to the projectile such that:

$$\left[\left(n-\frac{1}{2}\right)(n-1)n\right]^{1/3} \leq n_c < \left[n\left(n+\frac{1}{2}\right)(n+1)\right]^{1/3},$$
$$l \leq \frac{n}{n_c}\, l_c < l+1 \qquad (9)$$

are accordingly taken to belong to the (n,l) quantum state. The accuracy this approximation has been studied in detail in ref. [7].

3 Results

3.1 Ne^{10+} + H(1s) collisions

Molecular calculations were carried out with a molecular basis of 310 OEDMs including the entry channel, all σ, π and, δ orbitals dissociating into Ne^{9+}(nl) + H^+ with n=4, 5,...,15, and Ne^{10+} + H(n=2). In the CTMC calculations we have considered 10^5 trajectories that were integrated up to $t_{max} = 500$ a.u. Total and partial cross sections are plotted in figs. 1-3. As also shown in [6], total cross sections calculated using a single microcanonical initial distribution (7) show a worse agreement with the molecular results than those obtained by using the hydrogenic initial distribution (8), and the comparison of our capture cross sections with the experimental data of [14] is satisfactory. The ionization process is also better represented by using the hydrogenic than the microcanonical one, which underestimates the cross section as a consequence of its incorrect behaviour at large distances, that are the most important in this process [11,12], Given the lack of alternative experimental or theoretical results for this system, we have performed close-coupling calculations in terms of a basis of spherical Bessel functions [18] for $E \geq$ 100 keV/amu [6] and the excellent agreement with the hydrogenic CTMC ionization confirms the accuracy of both sets of results.

We have also analyzed in ref. [7] the behaviour of the CTMC partial cross sections, and we have explained that populations of low n ($n < 7$) levels are understimated with the hydrogenic distribution, although the method is accurate for high n levels, as those required in the diagnostics applications. In fig. 2, we have plotted our recommended data for this application, where, for $E < 30$ keV/amu (see vertical dotted line in fig. 2), we have applied the close-coupling formalism, and the CTMC for $E > 30$ keV/amu. At low-E, and

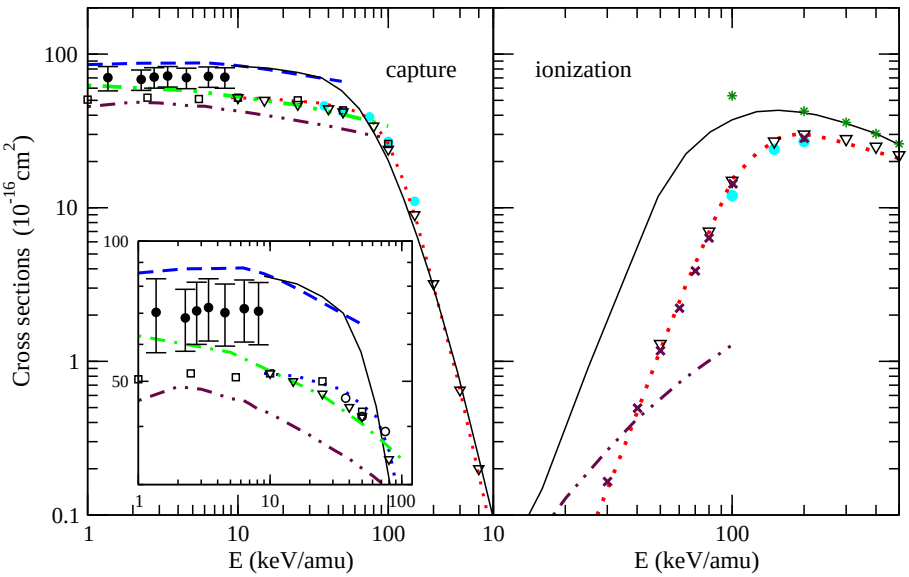

Fig. 1. Total capture (left) and ionization (right) cross sections in Ne^{10+}+H(1s) collisions as a function of the impact energy E. – – – Present molecular results; Present CTMC results: ——, hydrogenic; · · · ·,microcanonical. Other CTMC calculations: (- · -), [8]; (•),[15]; (□) [17]; ▽, [13]; (×), [20]. (∗), spherical Bessel monocentric expansion. (- · · -), hidden crossing [20]. Experimental results: •, [14] .

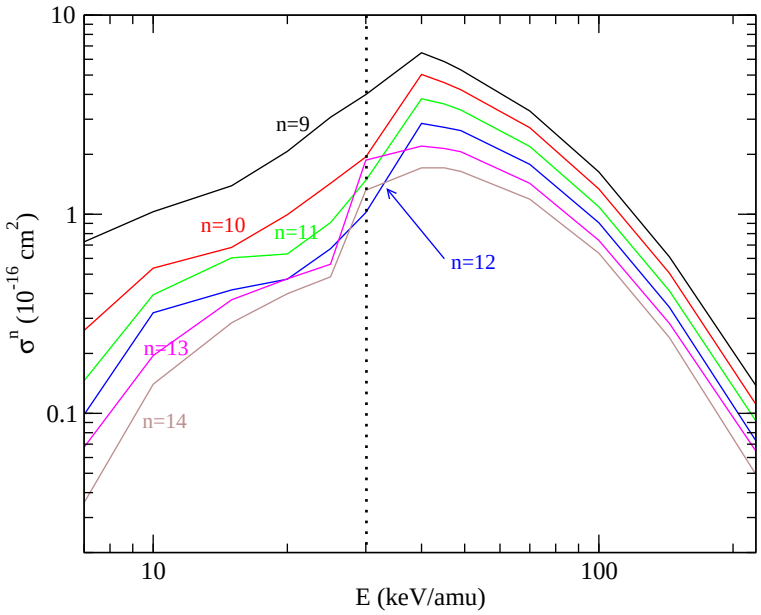

Fig. 2. Partial capture cross sections in Ne^{10+}+H(1s) collisions for the n-levels indicated in the figure.

for high n levels, interference effects lead to the oscillatory behaviour of partial cross sections in fig. 2. On the other hand, we have checked that, at sufficient large nuclear velocities ($E \gtrsim 100$ keV/amu), the empirical Oppenheimer n^{-3} rule [16], that is often employed to extrapolate the cross sections for high n values, applies to our data [6].

As an illustration, we show in fig. 3 the l distribution of the ($n = 10$) partial cross section. As for the case of n distributions, we find oscillatory l-distributions for $E < 30$ keV/amu , while, for higher energy collisions they show in general a single maximum at $l_{max} \simeq n - 2$ for $n < Z$=10 and $l_{max} \simeq 6 - 7$ for higher n.

3.2 Ar^{18+} + H(1s) collisions

Molecular calculations were carried out with a molecular basis of 271 OEDMs correlating to the entry channel and all σ, π and, δ orbitals dissociating into Ar^{17+}(nl) + H^+ with n=7, 8,..,15. In the CTMC calculations we have considered 10^5 trajectories that were integrated up to $t_{max} = 500$ a.u.. Total and partial cross sections are plotted in figs. 4-5. As in previous calculations, we find that the eikonal CTMC calculation using a single microcanonical distribution agrees with the 3-body calculations with the same distribution and both calculations underestimate the total capture cross section at low velocities, where the close-coupling calculation is expected to be more accurate. However, our improved CTMC results for total capture cross sections agree very well with the OEDM ones. On the other hand, the classical calculations for ionization exhibit a similar behaviour to that found for Ne^{10+}-H collisions (1), and as in previous calculations for collisions of ions with lower charge [12].

Although our molecular basis yields converged values of the total capture cross section, the evaluation of partial cross section would require a larger basis, in particular to obtain accurate values for the highest n levels. Accordingly, we only present in fig. 5 our classical results of the partial cross sections for those levels relevant in plasma diagnostics, and we have also plotted these cross sections for impact energies higher than those in fig. 2.

4 Concluding remarks

We have applied impact parameter molecular close-coupling and CTMC methods to evaluate electron capture and ionization cross sections; this allows us to cover a wide range of energies of interest in fusion diagnostic. The new data for Ne^{10+} + H (1s) collisions are now available in ADAS (see http://adas.phys.strath.ac.uk), and we have presented here an illustration of them, in particular for the partial electron capture cross sections of interest in diagnostics. We have also presented new data for Ar^{18+}+H(1s). As in previous calculations, we have obtained a noticeable improvement with respect to the widely used microcanonical distribution by employing the hydrogenic one. We have checked that for sufficient large collision energies, the n-partial cross

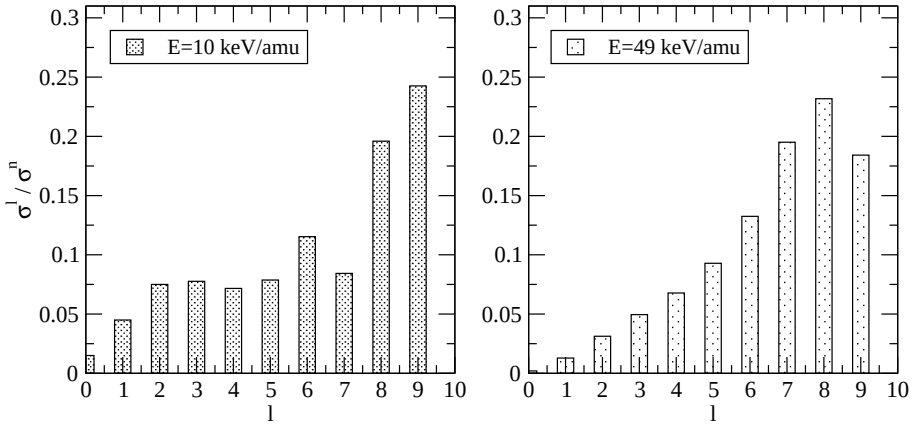

Fig. 3. l distribution of Ne^{9}+(n=10) formed in Ne^{10+}+H(1s) at the two impact energies indicated in the figure.

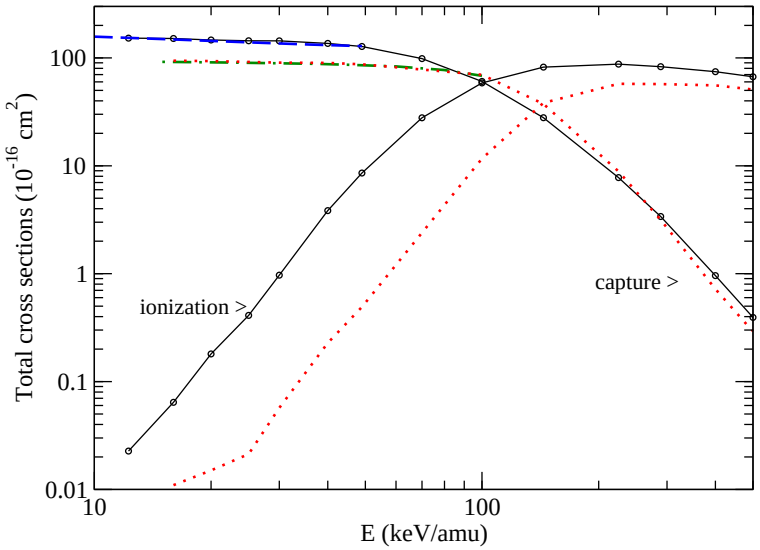

Fig. 4. Total capture and ionization cross sections in Ar^{18+}+H(1s) collisions as a function of the impact energy E. – – – , present molecular results. Present CTMC results: ——, hydrogenic; · · · ·, microcanonical. (- · -), microcanonical results for capture from ORNL (www-cfadc.phy.ornl.gov/eprints/argon.html)

sections verified the empirical Oppenheimer n^{-3} rule [16], for both collision systems. Further work is required to evaluate accurate partial cross sections for this system at low energies ($E < 20$ keV/amu). Also calculations are in progress to evaluate capture cross sections for the collisions with H(2s), since the presence of metastable H in the beam can strongly influence diagnostics experiments [10].

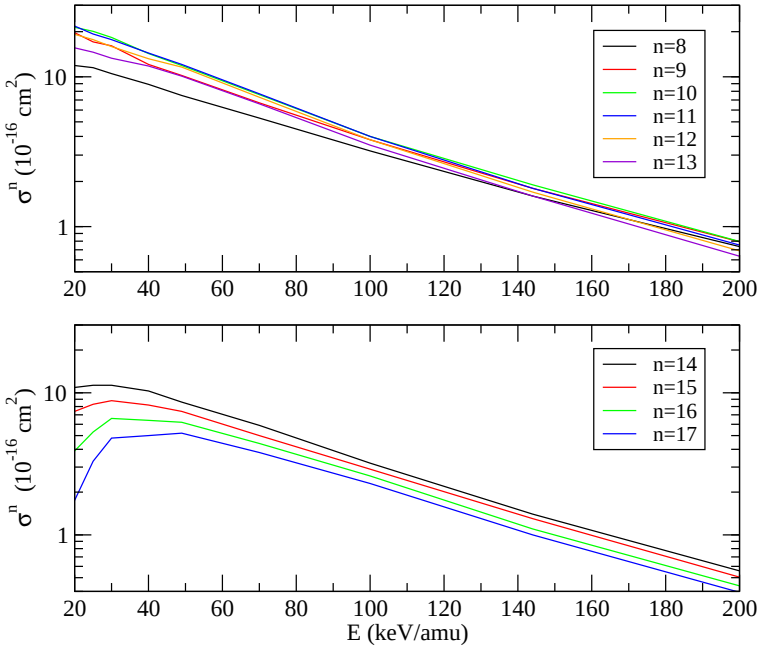

Fig. 5. Partial capture cross sections in Ar^{18+}+H(1s) collisions for the n-levels indicated in the figure.

5 Acknowledgments

This work has been partially supported by DGICYT projects BFM2000-0025 and FTN2000-0911. We would like to acknowledge the Ministerio de Ciencia y Tecnología (Spain) and the Ministère des Affaires Etrangères (France) for financial support under the coordinated program AIHF04-Picasso2004. CI acknowledges UAM for support under a research contract.

References

[1] R. Abrines and I. C. Percival. *Proc. Phys. Soc.*, 88:861, 1966.

[2] R. L. Becker and A. D. MacKellar. *J. Phys. B: At. Mol. Phys.*, 17:3923, 1984.

[3] B. H. Bransden and M. H C. McDowell. *Charge Exchange and the Theory of Ion-Atom Collisions*. Oxford, Clarendon, 1992.

[4] L. F. Errea, C. Harel, H. Jouin, J. M. Maidagan, L. Méndez, B. Pons, and A. Riera. *Phys. Rev. A*, 46:5617, 1992.

[5] L. F. Errea, C. Harel, H. Jouin, L. Méndez, B. Pons, and A. Riera. *J. Phys. B: At. Mol. Opt. Phys.*, 27:3603, 1994.

[6] L. F. Errea, C. Illescas, L. Méndez, B. Pons, A. Riera, and J. Suárez. *J. Phys. B: At. Mol. Opt. Phys.*, page submitted, 2004.

[7] L. F. Errea, C. Illescas, L. Méndez, B. Pons, A. Riera, and J. Suárez. *Phys. Rev. A*, page submitted, 2004.

[8] T. P Grozdanov. *J. Phys. B: At. Mol. Opt. Phys.*, 13:3835, 1980.

[9] D. J. W. Hardie and R. E. Olson. *J. Phys. B: At. Mol. Phys.*, 16:1983, 1983.

[10] R. Hoekstra, H. Anderson, F. W. Bliek, M. von Hellerman, C. F-Maggi, R. E. Olson, and H. P. Summers. *Plasma Phys. Control. Fusion*, 40:1541, 1998.

[11] C. Illescas, I. Rabadán, and A. Riera. *Phys. Rev. A*, 57:1809, 1998.

[12] C. Illescas and A. Riera. *Phys. Rev. A*, A60:4546, 1999.

[13] G. Maynard, R. K. Janev, and K. Katsonis. *J. Phys. B: At. Mol. Opt. Phys.*, 25:437, 1992.

[14] F. W. Meyer, A. M. Howald anc C. C. Havener, and R. A. Phaneuf. *Phys. Rev. A*, 32:3310, 1985.

[15] R.E. Olson and A. Salop. *Phys. Rev. A*, 16:631, 1977.

[16] J. R. Oppenheimer. *Phys. Rev.*, 31:349, 1928.

[17] J. A. Perez, R. E. Olson, and P. Beiersdofer. *J. Phys. B: At. Mol. Opt. Phys.*, 34:3063, 2001.

[18] B. Pons. *Phys. Rev. Lett.*, 84:4569, 2000.

[19] J. D. Power. *Phil. Soc. Trans. R. Soc*, 274:663, 1973.

[20] D. R. Schultz and P. S. Krstić. *At. and Plasma-Material Interaction Data for Fusion*, 6:173, 1996.